VARIABILITY OF SILICA FUME CONCRETE AND ITS EFFECT ON SEISMIC SAFETY OF REINFORCED CONCRETE BUILDINGS

Kirtikanta Sahoo[1]; Prateek Kumar Dhir[2*]; Peri Raghav Ravi Teja[3]; Pradip Sarkar[4]; and Robin Davis[5]

[1]Assistant Professor, Department of Civil Engineering, KIIT University, Bhubaneswar, India. Email: sahoo.kirti@gmail.com.

[2*]Ph. D. Scholar at Department of Civil and Environmental Engineering, University of Strathclyde, Glasgow, UK, Email: prateek.dhir@strath.ac.uk (corresponding author)

[3] M. Tech. Scholar at Department of Civil Engineering, National Institute of Technology, Rourkela, India, 769008, India. Email: prraviteja04@gmail.com.

[4]Associate Professor, National Institute of Technology, Rourkela, India, 769008, Email: sarkar.pradip@gmail.com.

[5]Assistant Professor, National Institute of Technology, Rourkela, India, 769008, Email: robin.davisp@gmail.com.

ABSTRACT

Design of structures made using Silica Fume (SF) concrete to an acceptable level of safety requires the probabilistic evaluation of its mechanical properties. An extensive experimental program was carried out on compressive strength, flexural strength and tensile splitting strength of SF concrete. Seven concrete mixes with different proportions of SF were designed to produce 490 concrete samples. The probabilistic models to describe the variability of the mechanical properties of SF concrete were proposed. Two parameter probability models such as Weibull, normal, lognormal and gamma distribution were considered for the representation of variability. The probability distribution models were selected based on the three goodness-of-fit tests such as the Kolmogorov-Sminrov (KS), Chi-square (CS) and log-likelihood (LK) tests. The results obtained from the models are useful for description of the variability of selected mechanical properties of SF incorporated concrete. This study proposed lognormal distribution function as the distribution model that most closely describes the variations of different mechanical properties of SF concrete for a practical point of view. Further, the performance of typically selected buildings using SF concrete was evaluated through fragility curves and reliability indices incorporating the proposed probability distributions and variability of compressive strength property. It was found that 15% to 25% of partial replacement of cement with SF may yield better performance of the frames.

Keywords: Variability, silica fume concrete, compressive strength, flexural strength, tensile splitting strength, fragility curve, seismic hazard curve, reliability curve

INTRODUCTION

Accumulations of industrial waste products create environmental problems and outline the need for their greater utilization in different fields. The construction field utilizes such materials by replacing it partially as a supplementary cementing material in concrete and contributes towards the sustainability. Supplementary materials like fly ash, SF, metakaolin and ground granulated blast furnace slag (Radonjanin *et al*. 2013) are used due to their pozzolanic activity and among them, SF is found to be highly operative in the design and development of concrete (Siddique 2011). The incorporation of SF concrete in the construction sector is gaining popularity in the recent years, which demands the design and safety assessment of these structures in the future. The structural performance and safety of any kind of structure is dependent on the uncertainty in the properties of materials. But, in reality, this phenomenon is ignored in conventional structural design and analysis. The assumption of the deterministic values of the material properties is less satisfactory and less realistic. Now a days due to advancement in technology, complex structural analyses like probablistic study can be easily performed by considering various uncertainty parameters of the structures and its response against the natural loads such as earthquake, wind etc.

Several studies (Campbell and Tobin 1967, Soroka 1968, Chmielewski and Konapka 1999, Graybeal and Davis 2008) have been performed on the variability of the compressive strength of concrete. The variability of compressive strength of concrete is usually represented in literature by a normal distribution if the coefficient of variation does not exceed 15-20%, although slight skewness may be present. However, when the coefficient of variation is high, the skewness is considerable (Campbell and Tobin 1967) and if the quality control is poor (Soroka 1968), a lognormal distribution is more rational to represent the tail areas of distribution than a normal distribution. A recent study (Chen *et al*. 2013) concludes that the variation in concrete compressive strength should be characterized using various statistical criteria and different distribution functions.

The inherent variability of cement and SF may not be similar in nature as it is a by-product in the carbothermic reduction of high-purity quartz with carbonaceous materials like coal, coke, wood-chips in the production of silicon and ferrosilicon alloys. Therefore, the existing literature on the variability of cement concrete may not be useful to describe the variability of concrete with SF. In the present study, different probability functions along with traditionally used normal and lognormal functions were implemented for the explanation of the variation of diverse mechanical properties of SF concrete obtained experimentally. A best-fitted probability distribution function for mechanical properties of concrete with different amount of SF is developed adopting various statistical tests. Further, the relative seismic vulnerability of buildings made with a specified percentage of SF is studied in comparison with a regular Reinforced Concrete (RC) buildings for a site hazard conditions in a practical load and resistance factor format.

RESEARCH SIGNIFICANCE

Performance-based analysis requires probabilistic distributions of the constituent materials in the structure. Though the variability in the mechanical properties associated with normal concrete is reported in the literature, however, most of the literature did not reveal about the variability of concrete made with partial replacement of SF. In this research, three important mechanical properties: compressive strength, flexural strength and tensile splitting strength of SF concrete were described through the probability distribution functions. Best fitted probability distribution function is developed by performing numerous goodness-of-fit tests. Further, the performance of typically selected buildings using SF incorporated concrete is evaluated through fragility curves and reliability indices incorporating the proposed probability distributions and variability of compressive strength of SF concrete. The development of probability description of the SF concrete and the seismic performance assessment of buildings built with SF incorporated concrete is a new research attempt in this study.

EXPERIMENTATION

The experimental program consists of seven sets of concrete mixes with partial replacement of SF. Most of the previous studies on SF concrete, consider the partial replacement of cement keeping the total weight of cementitious material, fine and coarse aggregate as constant values. The main purpose of these studies was to evaluate the effect of SF on the behavior of concrete. International codes like Indian Standard, IS10262 (2009) and ACI 234R (96) recommends an extra cement of 10%, while mineral admixture like silica fume is used as partial replacement of cement. The present study focuses on the variability of mechanical properties SF incorporated concrete and its effect on the seismic performance of SF incorporated (as per the above codes) RC frames. Weight proportions of cement, SF, natural sand, coarse aggregates, water and admixture for all the seven mixes are shown in Table 1. The cement content in the control mix is found to be about 308 kg/m^3, while the total cementitious content, in the mixtures where the replacement of SF is carried out, is kept constant at about 338kg/m^3 (1.10 times of the cement content of the control mix) as per IS 10262 (2009). As the percentage of SF increase the cement contents in SF concrete mixtures reduces from 322 kg/m^3 (5% SF) to 237 kg/m^3 (30% SF). The doses of SF are 0% (control mix), 5%, 10%, 15%, 20%, 25%, and 30% of the total cementitious material (Atiş *et al.* 2005, Poon *et al.* 2006). Water content is kept constant as 148kg/m^3 [9.239lb/ft^3], maintaining maximum doses of superplasticizer as 1.3% of cement weight. Portland Slag Cement having the 28-day compressive strength of 48 MPa [6.96 ksi] and SF of grade 920-D having a specific surface area of about 19.5 m^2/kg [95.22 ft^2/lb] were used in this study. The chemical and physical properties of cement and SF were analyzed and found to be conforming to the relevant standard (ASTM C989/C989M-14 for cement and ASTM C1240 for SF) and shown in Table 2 & 3. The specific gravity of cement and SF were found to be 3.01 and 2.26 respectively. Natural river sand conforming to Zone-II of IS 383 (1970) was used as fine aggregate. Specific gravity and water absorption of fine aggregates were obtained as 2.65 and 0.8%, respectively. Crushed angular graded coarse aggregate obtained from a local quarry having a nominal maximum size of 20 mm [0.78 inches] was used. The specific gravity and the water absorption of the coarse aggregates were 2.75 and 0.6 % respectively.

Test specimens (Cube size: 100mm x 100mm x 100mm, Cylinder size: 100mm x 200mm, Prism size: 100mm x 100mm x 500mm) were prepared from each of the seven mixes for compressive strength, tensile splitting strength and flexural strength test. The specimens were casted in a weather condition where the ambient temperature range was about 21^{0}C to 45^{0}C and humidity range was about 47% to 63%. The curing was carried out in water filled tank located adjacent to the laboratory for 28 days.

Variability in Mechanical Properties

All the specimens mentioned in the previous section were tested according to relevant Indian Standards. Individual test results, including the associated mean and standard deviation for compressive strength, flexural strength, and split tensile strength respectively in the Tables 1A to 3A (in the APPENDIX).

The compressive strength of concrete cubes (7 mixes × 30 samples each = 210 total samples) with various SF content is presented in Table 4. The compressive strength of control specimen was found to be varying from 24.18 MPa [3.50 ksi] to 34.60 MPa [5.01 ksi] with a mean and Standard deviation (SD) of 30.27 MPa [4.38 ksi] and 2.17 MPa [0.314 ksi]. Similarly, the minimum, maximum, mean and SD for other concrete specimens having a different percentage of SF is shown in this table. The mean compressive strength of concrete increases with SF content and it reaches maximum value 53.97 MPa [7.825 ksi] at 20% SF content. The table also shows that the SD of compressive strength increases with the increase in SF content. This may be attributed to the high inherent variability in the properties of SF. The mean compressive strengths of concrete obtained for each SF dosage are plotted in Fig. 1.

Flexural strength of concrete prisms (7 mixes × 20 samples each = 140 total samples) with various SF content is presented in Table 4. The flexural strength of control specimen is varying from 5.94 MPa [0.86 ksi] to 6.41 MPa [0.92 ksi] with a mean and SD of 6.32 MPa [0.91 ksi] and 0.33 MPa [0.04 ksi]. Similarly, the minimum, maximum, mean and SD for other concrete specimens having a different percentage of SF is presented in Table 4. The mean flexural strength of concrete increases with SF content and it reaches maximum value 8.35 MPa [1.21 ksi] at 25% SF content. It can be seen from this table that the SD values of concrete follow the non-uniform trend with the increase in SF content. The mean flexural strength of concrete obtained for each SF dosage is plotted in Fig. 2.

The tensile splitting strengths of the concrete cylinder (7 mixes × 20 samples each = 140 total samples) with various SF contents are presented in Table 4. The tensile splitting strength of the control specimen varies from 2.21 MPa [0.32 ksi] to 2.96 MPa [0.42 ksi] with a mean and SD of 2.60 MPa [0.37 ksi] and 0.23 MPa [0.3 ksi] respectively. Similarly, the minimum, maximum, mean and SD for other concrete specimens having a different percentage of SF is shown in Table 4. The mean tensile splitting strength of concrete increases with SF content and it reaches a maximum value of 3.91 MPa [0.56 ksi] at 20% SF replacement. This table shows that the SD of tensile splitting strength increases with the increase in SF content. The mean tensile splitting strengths of concrete obtained for each SF dosage are plotted in Fig. 3.

Development of Variability Models

Design and safety assessment of structures made of silica fume concrete requires probabilistic models that describe the variability of its mechanical properties. This section focuses on the representation of variability of compressive strength, flexural strength and tensile splitting strength using different probability distribution models. Values of all the mechanical properties obtained experimentally were converted to probability distribution functions using the shape and scale parameters obtained from the sample data (e.g. for normal distribution: shape and scale factor implies the mean and standard deviation values respectively). Certain pre-decided standard probability distribution models selected in the present work are; truncated normal, lognormal, gamma and Weibull distributions. Certain statistical goodness-of-fit tests (Chen *et al*. 2013) like as modified Kolmogorov-Smirnov (KS), Log-likelihood (LK) and minimum Chi-square criterion (CS) at the 5% significance level were performed. The probability distribution which has minimum values of KS distance and CS value and the maximum value of LK was considered as the best fit. These methods have been successfully used in many past works of literature (Chen *et al*. 2013, Stone *et al*. 1986).

The distribution is rejected if the goodness-of-fit test values are below the critical value specified at the 5% significance level. The values obtained for the rejected distributions were omitted in the presentation of results. The selection criteria for a best-fit distribution is the minimum values of KS distance and CS along with the maximum value of LK. The CS value may not be always reliable (Chen *et al*. 2013) because it depends on the binning of data into intervals and it is best suitable when large random variables are used. Therefore, the best-fitted distribution was decided from KS distance and LK value even if the CS value is not the minimum.

The estimated parameter values of different distributions for compressive strength, flexural strength and tensile splitting strength are reported in Tables 5, 6, and 7 respectively. The graphical representation of cumulative probability distributions from experiments was compared with assumed distribution functions for all data sets as shown in Figs. 4-6.

Statistical Inference for compressive strength, flexural strength and tensile splitting strength

The parameters (KS distances, LK and CS values) of the goodness-of-fit tests for the mechanical properties, compressive strength, flexural strength and tensile strength are shown in Table 5-7 respectively. The three criteria (KS, CS and LK) were found to be not in agreement simultaneously to choose a single probability distribution for a variability description of compressive strength. However, there are negligible deviations among the goodness-of-fit test values for all the cases of mix proportions. A single probability distribution was found to satisfy all the test criteria to yield the minimum KS distance, minimum CS and maximum LK value for a mix with 10%, 15% and 20% SF replacement. Accordingly, Lognormal and Weibull distribution were found to be the best fit models for mix with 10%, 15% and 20% SF respectively.

However, for mix with 0%, 5%, 25% and 30% SF, no single distribution meets all the test criteria but the values of all distributions are close to each other. Therefore, depending on KS distance and LK value, either Lognormal or the Weibull seems to be the closest fit model for these concrete mixes. For flexural strength, mix with 5%, 15% and 20% SF, Weibull distribution meets all the selecting criteria. Similarly, for mix with 30% SF, lognormal distribution meets all the test criteria. However, no single distribution meets all the selecting criteria for mix with 0%, 10% and 25% SF. Based on KS and LK values, either of Weibull or lognormal distribution can be considered as the close fit distribution for these mixes. Similarly, for tensile strength, mix with 0%, 15% and 30% SF, a single distribution meets all the selecting criteria. Hence, lognormal, Gamma and Gamma distributions were found to be the best fit models for mix with 0%, 15% and 30% SF respectively. No single distribution meets all the selecting criteria for mix with 5%, 10%, 20% and 25% SF. The probability distributions generated from the experimental results and the cumulative probability distribution models for compressive strength, flexural strength and tensile strength of SF concrete for different mix proportions of SF are shown in Figs. 6-8. The appropriate statistical distribution functions (with their respective shape and scale parameters) obtained for different mechanical properties of silica fume concrete are summarized in Table 8. It can be seen from this table that Weibull and Lognormal distribution function describe the variation of different mechanical properties of silica fume concrete most agreeably.

PROBABILITY DISTRIBUTION MODEL AND SEISMIC FRAGILITY CURVES

Having established the probabilistic representations of the variability in the mechanical properties of the SF concrete, it is prudent to study the effect of the proposed probability distributions of compressive strength in the performance of buildings through seismic fragility curves and reliability curves for the prediction of seismic performance of buildings constructed using SF concrete. A simplified method by Ellingwood (2001) was adopted in the present study for the development of fragility curves.

The seismic hazard curve, $G_A(x)$, a plot of $P\,[A = a]$ and the magnitude of ground acceleration (a). The limit state probabilities of achieving a series of progressively severe stages, LS_i, are expressed as follows;

$$P[LS_i] = \sum_a P[LS_i \mid A = a]P[A = a] \quad \text{(Eq. 1)}$$

The uncertainty in the above equation is referred as the seismic fragility, $F_R(x)$ and observed to follow a two parameter lognormal probability distribution (Song and Ellingwood 1999; Cornell *et. al.* 2002; Haran 2014 and Haran *et. al.* 2015). A point estimate of the LS_i of state *i* can be calculated by combining the $F_R(x)$ with the derivative of $G_A(x)$, thus removing the acceleration condition,

$$P[LS_i] = \int F_R(x)\frac{dG_A}{dx}dx \quad \text{(Eq. 2)}$$

The reliability index conforming to the failure probability can be predicted by the following standard equation;

$$\beta_{Pf} = -\phi^{-1}(P[LS_i]) \quad \text{(Eq. 3)}$$

Where ϕ ( ) represents the standard normal distribution.

At moderate to large ground accelerations, a linear logarithmic relation exists between the annual probability of occurrence and the spectral acceleration. The hazard equation, *GA(a)*, suggested by Ellingwood (2001) can be described as follows;

$$G_A(x) = 1 - \exp[-(x/u)^{-k}] \quad \text{(Eq. 4)}$$

where, *u* and *k* are the distribution parameters.

Nath and Thingbaijam (2012), Pallav *et al*. (2012), Raju *et al.* (2012) and Sitharam *et al.* (2015) have developed the seismic hazard curves for India and few studies (Iyengar *et al*. 2010 and Dhir *et al*. 2018) have considered the seismic hazard curves available at the National Disaster Management Authority for the seismic hazard analysis. In this study, seismic hazard curve of Imphal was selected (Fig. 7) being the most vulnerable location in seismic Zone V of India.

FRAME CONSIDERED

A typical RC bare frame having four stories (uniform story height of 3.2m) and two bays (uniform bay width of 5m) was considered. This building was designed for seismic force corresponding to highest seismic Zone V (Peak Ground Acceleration of 0.36g) as per IS 1893 (2002) and considering medium soil conditions (N-value in the range 10-30). The characteristic strength of concrete and steel were considered as 25 MPa and 415 MPa, respectively. As the building is symmetric in plan and elevation, a single plane frame was considered to be representative of the building along the loading direction. The dead load of the slab and the live load on it were considered as 0.00375 MPa and 0.003 MPa respectively. The self-weight of the partition walls (230 mm) was applied separately as the uniformly distributed load on the respective beams and the design base shear was estimated using the equivalent static method as per IS 1893 (2002).

In order to study the effect of variability in the compressive strength properties of concrete made by the partial replacement of cement by SF, different building models were considered to represent various practical cases with varying percentage of SF. Buildings were named as XY, where X denotes 'SF' for silica fume. Y denotes the percentage of replacement of SF. The building frame with normal reinforced concrete was represented as 'C'. Fig. 8 shows the configuration of four storey two bay frame and Table 9 shows the design details of the selected frame.

Structural Modelling

Selected buildings were modelled for nonlinear time history analysis needed for the seismic risk assessment. The Open System for Earthquake Engineering Simulation (OpenSEES) Laboratory tool developed by McKenna *et al.* (2014) was considered for all the analysis. A force-based nonlinear beam-column fiber element that considers the spread of plasticity along the element was used for modelling the beams and columns for nonlinear time history analysis. Formulation of the force-based fiber element was explained in Lee and Mosalam (2004). Kunnath (2007) has studied the sensitivity due to the number of integration points in each element and suggested the use of five integration points for nonlinear analysis of fiber elements, which was followed in the present study. The modelling of the core concrete performed by bearing in mind the influence of the special reinforcement detailing in the beams and columns suggested by Kent and Park

(1971) and the cover concrete was modelled as unconfined concrete. Giuffre- Menegotto-Pinto steel material model was used for the modelling of steel reinforcing bars. Details of reinforcement modelling are available in Filippou *et al.* (1983).

In the current study, a lumped mass approach was taken in which all the permanent weights that move with the structure is lumped at the suitable nodes. It comprises of all the dead loads and part of the live load (25%) that are expected to be present in the structure during the ground shaking. The in-plane stiffness of the floor was modelled using rigid diaphragm constraint. Damping was modelled using Raleigh damping for dynamic analysis, reported by Filippou *et al.* (1992). In this study, 44 ground motions (22 pairs) were considered (Haselton *et al.* 2012) and the details of the same are available in Haran *et al.* (2015). These ground motions were converted to match with IS 1893 (BIS 2002) design spectrum using a computer program (Mukherjee and Gupta 2002) and used for the nonlinear dynamic analyses. Uncertainties associated with concrete compressive strength, the yield strength of reinforcing steel, and global damping ratio were considered in the probabilistic seismic risk assessment. The mean value and coefficient of variation (COV) of the normal probability distributions of the above parameters (uncorrelated) were obtained from published literature and presented in Table 10. Details of random variables used and assumptions of the computational modelling are available in Dhir *et al.* (2018).

Development of Fragility Curves

The fragility function represents the probability of exceedance of a selected Inter Storey Drift (*ISD*) for a selected structural limit state (*LS*) for a specific ground motion Peak Ground Acceleration (*PGA*) and the seismic fragility, $F_R(x)$ can be expressed as follows,

$$P(D \geq C \mid \mathrm{PGA}) = \varphi\left(\frac{\ln \frac{S_D}{S_C}}{\sqrt{\beta_{D|\mathrm{PGA}}^2 + \beta_c^2}}\right) \quad \text{(Eq. 5)}$$

where, C is the drift capacity at chosen limit state and D is the drift demand, S_C and S_D are the median of the chosen limit state (*LS*) and the demand respectively. β_c and $\beta_{d/PGA}$ are dispersions in the capacities and

PGA respectively. β_c is dependent on the construction quality and the building type considered. Depending on the quality of construction, the values of β_c can be 0.10, 0.25 and 0.40 as good, fair and poor respectively (ATC 58 2012) and in the present study it is assumed as 0.25. Many researchers (Nielson *et. al.* 2005; Davis *et. al*. 2010b; Rajeev and Tesfamariam 2012; Haran 2014, Haran *et. al.* 2015, Bhosale 2016, 2017, 2018; Dhir *et al*. 2018) have implemented this methodology to develop fragility curves of RC structures and its correctness has also been validated.

Probabilistic Seismic Demand Model (PSDM)

PSDMs for nonlinear time history analysis are given in terms of a suitable PGA. Cornell *et.al* (2002) suggested that the estimation of the median demand, $ISD(S_D)$ can be calculated in a generalized equation (a power model) as per in Eq. 6.

$$ISD = a\left(PGA\right)^{b} \qquad \text{(Eq. 6)}$$

Where, *a* and *b* are the regression coefficients obtained from PSDMs.

Performance limit states

Limit states define the capacity of the structure to withstand different levels of damage. The median inter-storey drift limit states for both RC moment resisting infilled and bare frame structures defining the capacity of the structure at various performance levels (S_C) are suggested by ASCE/SEI 41-06 (2007). Drift limits for RC frames as per ASCE/SEI 41-06 (2007) are considered in the present study as 2% and 4% for significant damage (SD) and near collapse (CP) performance levels respectively.

Material uncertainty

The most sensitive random variables such as compressive strength of concrete, yield strength of steel and global damping ratio in a constructed building frame were considered as random. The mean and standard deviations (in terms of COV) of all the random variables are presented in Table 11. Using Latin Hypercube sampling technique, a set of 44 values was produced to generate 44 computational models for conducting the nonlinear dynamic analysis.

PSDMs for all frames

The 44 earthquake ground motions were linearly scaled from 0.1g to 1g and each 44 computational models were analysed for a particular randomly selected earthquake with a particular PGA. The inter-storey drifts (maximum of all storeys) with the corresponding PGAs were plotted on a logarithmic graph for buildings with SF concrete as shown in Fig. 9. Using regression analysis, a power law (refer to Eq. 6) relationship for each frame, was fitted which represents the PSDM model for the corresponding frames. Higher the value of inter-storey drifts, the higher will be the vulnerability of the building. The regression coefficients '*a*' and '*b*', of the PSDMs, are found for each frame and reported in Table 12.

Fragility Curves

In order to study the performance of selected cases of building frames, the fragility curves are developed for all the frames for each performance limit states as shown in Fig. 10 for SF frames. Figs. 10a and 10b show the fragility curves at SD and CP performance levels respectively for SF frames. It can be seen from Figs. 10a and 10b that the SF frames with 15%, 20% and 25% partial replacement of SF was found to be performing better than other frames for all performance limit states.

Comparison of reliability indices

In order to understand the performance of each frame quantitatively, the seismic reliability indices were calculated for each frame. The reliability indices were estimated by combining the fragility curve for a particular limit state and site seismic hazard curve (Eq. 2). In the present study, the hazard curve of North East India was chosen for reliability index estimation. Reliability index was calculated for two performance objectives, PO-II and PO-III, namely, Significant Damage (SD) performance level at an earthquake having a 10% probability of occurrence in 50 years (PO-II) and Collapse Prevention (CP) performance level at an earthquake having a 2% probability of occurrence in 50 years (PO-III). PGAs at 10% and 2% probability of occurrence were obtained from the hazard curve (Fig. 7) as 0.67g and 1.35g respectively. Reliability indices for different performance levels in terms of various PGA values are presented in Fig. 11 for SF buildings. Figs. 11a and 11b show the variation of reliability indices for different PGAs for all SF frames at SD and CP performance levels respectively. The PGAs corresponding to PO-II and PO-III performance levels are marked in these figures for the calculation of reliability indices at each performance objectives.

The reliability indices of all frames at PO-II and PO-III performance objectives are tabulated in Table 13. The seismic reliability of the SF concrete frames depends on many parameters including the statistics of the compressive strength of the SF concrete. Although it cannot be generalised, in order to understand the trend of the variation of seismic reliability at the two performance levels with the variation of replacement ratio of SF, a plot of normalised reliability (ratio of the seismic reliability index of the SF frames to the seismic reliability index of control frame) as shown in the Fig. 12 was considered. The equations representing the trend of the variation of the normalised reliability index with the variation of the SF ratio for the two performance objectives (PO-II and PO-III) and the corresponding coefficient of determination (R^2). The trend shows that the normalised seismic reliability index increases (for both PO-II and PO-III) initially, reaches an optimum at about 15 to 25% and then decreases with SF replacement ratio. Therefore, addition of SF in the range of 15% to 25% may yield better seismic performance.

SUMMARY AND CONCLUSIONS

The study of the statistical variations was carried out using the experimental data and considering several two parameter probability distribution functions with an aim to describe the variability of the mechanical properties of SF concrete. Several two-parameter distributions were selected to find the best-fit model that describes the experimental data closely. Based on the limited set of data and using three goodness-of-fit tests (minimum KS distance, minimum CS and maximum LK values), most appropriate statistical distributions for the selected parameters were proposed. The three selected statistical criteria (KS, CS and LK) are not always found to be in agreement with a single distribution for some of the concrete mixes. In such cases, the closest fit model was selected based on the KS distance and LK value (Chen *et al*. 2013). For other mixes, a single distribution was found to meet all the three validating criteria. This study proposed lognormal distribution function as the probability distribution model that most closely describes the variations of different mechanical properties of SF concrete from a practical viewpoint. Further, the performance of typically selected buildings using SF concrete was evaluated through fragility curves and reliability indices incorporating the proposed probability distributions and variability of material properties. It was found that 15% to 25% of partial replacement of cement with SF may yield better performance of the frames.

REFERENCES

ACI 234R-96 (Reapproved 2000), Guide for the Use of Silica Fume in Concrete, Reported by ACICommittee 234.

Applied Technology Council (ATC-58). (2007). Guidelines for Seismic Performance Assessment of Buildings.

ASCE/SEI Seismic Rehabilitation Standards Committee. (2007). Seismic rehabilitation of existing buildings (ASCE/SEI 41-06). *American Society of Civil Engineers, Reston, VA*.

ASTM, A. (2011). Standard specification for silica fume used in cementitious mixtures.

ASTM. (2012). Standard specification for slag cement for use in concrete and mortars.

Atiş, C. D., Özcan, F., Kılıc, A., Karahan, O., Bilim, C., & Severcan, M. H. (2005). Influence of dry and wet curing conditions on compressive strength of silica fume concrete. *Building and environment*, *40*(12), 1678-1683.

Bhosale, A. S., Davis, R., & Sarkar, P. (2017). Vertical irregularity of buildings: Regularity index versus seismic risk. *ASCE-ASME Journal of Risk and Uncertainty in Engineering Systems, Part A: Civil Engineering*, *3*(3), 04017001.

Bhosale, A. S., Davis, R., & Sarkar, P. (2018). Seismic Safety of Vertically Irregular Buildings: Performance of Existing Indicators. *Journal of Architectural Engineering*, *24*(3), 04018013.

Bhosale, A., Davis, R., & Sarkar, P. (2016). Sensitivity and Reliability Analysis of Masonry Infilled Frames. *World Academy of Science, Engineering and Technology, International Journal of Civil, Environmental, Structural, Construction and Architectural Engineering*, *10*(12), 1531-1535.

BIS (Bureau of Indian Standards). (2002). "Criteria for earthquake resistant design of structures. Part 1: General provisions and buildings." IS-1893, New Delhi, India.

BIS, I. (2002). Criteria for Earthquake Resistant Design of Structures Part 1 General Provisions and Buildings. *Bureau of Indian Standards, Fifth revision*.

Campbell, R. H., & Tobin, R. E. (1967, April). Core and cylinder strengths of natural and lightweight concrete. In *Journal Proceedings* (Vol. 64, No. 4, pp. 190-195).

Celik, O. C., & Ellingwood, B. R. (2009). Seismic risk assessment of gravity load designed reinforced concrete frames subjected to Mid-America ground motions. *Journal of Structural Engineering*, *135*(4).

Celik, O. C., & Ellingwood, B. R. (2010). Seismic fragilities for non-ductile reinforced concrete frames–Role of aleatoric and epistemic uncertainties. *Structural Safety*, *32*(1), 1-12.

Chen, X., Wu, S., & Zhou, J. (2013). Variability of compressive strength of concrete cores. *Journal of Performance of Constructed Facilities*, *28*(4), 06014001.

Chmielewski, T., & Konopka, E. (1999). Statistical evaluations of field concrete strength. *Magazine of concrete research*, *51*(1), 45-52.

Cornell, C. A., Jalayer, F., Hamburger, R. O., & Foutch, D. A. (2001). The probabilistic basis for the 2000 SAC/FEMA steel moment frame guidelines. Submitted to. *J. Struct. Engrg*.

Davis, P. R., Padhy, K. T., Menon, D., & Prasad, A. M. (2010, July). Seismic fragility of open ground storey buildings in India. In *9th US National and 10th Canadian Conference on Earthquake Engineering*.

Dhir, P. K., Davis, R., & Sarkar, P. (2018). Safety Assessment of Gravity Load–Designed Reinforced Concrete–Framed Buildings. *ASCE-ASME Journal of Risk and Uncertainty in Engineering Systems, Part A: Civil Engineering*, 4(2), 04018004.

Ellingwood, B. R. (2001). Earthquake risk assessment of building structures. *Reliability Engineering & System Safety*, *74*(3), 251-262.

Filippou, F. C., D'ambrisi, A., & Issa, A. (1992). *Nonlinear static and dynamic analysis of reinforced concrete subassemblages*. Earthquake Engineering Research Center, College of Engineering, University of California.

Ghobarah, A. (2001). Performance-based design in earthquake engineering: state of development. *Engineering structures*, *23*(8), 878-884.

Graybeal, B., & Davis, M. (2008). Cylinder or cube: strength testing of 80 to 200 MPa (11.6 to 29 ksi) ultra-high-performance fiber-reinforced concrete. *Materials Journal*, *105*(6), 603-609.

Haran, P. D. C. (2014). "Reliability based seismic design of open ground storey framed buildings." Ph.D. thesis, National Institute of Technology Rourkela, Rourkela, Orissa, India.

Haran, P. D. C., Bhosale, A., Davis, R. P., and Sarkar, P. (2016). "Multiplication factor for open ground storey buildings: A reliability based evaluation." *Earthquake Eng. Eng. Vibr.*, 15(2), 283–295.

Haran, P. D. C., Davis, R. P., and Sarkar, P. (2015). "Reliability evaluation of RC frame by two major fragility analysis methods." *Asian J. Civ. Eng.*, 16(1), 47–66.

Haselton, C. B., Whittaker, A. S., Hortacsu, A., Baker, J. W., Bray, J., & Grant, D. N. (2012, September). Selecting and scaling earthquake ground motions for performing response-history analyses. In *Proceedings of the 15th World Conference on Earthquake Engineering*.

IS: 383. (1970). Specification for coarse and fine aggregates from natural sources for concrete.

Iyengar, R. N., Chadha, R. K., Rao, K. B., and Raghukanth, S. T. G. (2010). "Development of probabilistic seismic hazard map of India." Final Rep., National Disaster Management Authority, New Delhi, India.

Kent, D. C., and Park, R. (1971). "Flexural members with confined concrete." *J. Struct. Div*., 97(7), 1969–1990.

Kunnath, S. K. (2006). *Application of the PEER PBEE Methodology to the I-880 Viaduct: I-880 Testbed Committee*. Pacific Earthquake Engineering Research (PEER) Center, College of Engineering, University of California.

Lee, T. H., & Mosalam, K. M. (2004). Probabilistic fiber element modeling of reinforced concrete structures. *Computers & structures*, *82*(27), 2285-2299.

McKenna, F., McGann, C., Arduino, P., & Harmon, J. A. (2013). OpenSEES laboratory.

Mukherjee, S., & Gupta, V. K. (2002). Wavelet-based generation of spectrum-compatible time-histories. *Soil Dynamics and Earthquake Engineering*, *22*(9-12), 799-804.

Nath SK, Thingbaijam KKS. Probabilistic Seismic hazard assessment of India, Seismological Research Letters, 2012:135-149.

Nielson, B. G. (2005). *Analytical fragility curves for highway bridges in moderate seismic zones* (Doctoral dissertation, Georgia Institute of Technology).

Pallav, K., Raghukanth, S.T.G. and Singh, K.D., (2012). Probabilistic seismic hazard estimation of Manipur, India. *journal of geophysics and engineering*, 9(5), p.516.

Poon, C. S., Kou, S. C., & Lam, L. (2006). Compressive strength, chloride diffusivity and pore structure of high performance metakaolin and silica fume concrete. *Construction and building materials*, *20*(10), 858-865.

Radonjanin, V., Malešev, M., Marinković, S., & Al Malty, A. E. S. (2013). Green recycled aggregate concrete. *Construction and Building materials*, *47*, 1503-1511.

Rajeev, P., & Tesfamariam, S. (2012). Seismic fragilities for reinforced concrete buildings with consideration of irregularities. *Structural Safety*, *39*, 1-13.

Raju KR, A Cinitha A, Iyer NR. Seismic performance evaluation of existing RC buildings designed as per past codes of practice, *Indian Academy of Sciences*, 2002: Vol. 37, No. 2, April 2012, pp. 281–297.

Ranganathan, R. (1999). *Structural reliability analysis and design*. Jaico Publishing House.

Siddique, R. (2011). Utilization of silica fume in concrete: Review of hardened properties. *Resources, Conservation and Recycling*, *55*(11), 923-932.

Sitharam, T. G., Kolathayar, S., & James, N. (2015). Probabilistic assessment of surface level seismic hazard in India using topographic gradient as a proxy for site condition. *Geoscience Frontiers*, *6*(6), 847-859.

Song, J., & Ellingwood, B. R. (1999). Seismic reliability of special moment steel frames with welded connections: II. *Journal of Structural Engineering*, *125*(4), 372-384.

Soroka, I. (1968). An application of statistical procedures to quality control of concrete. *Materials and Construction*, *1* (5), 437-441.

Standard, I. (2004). Recommended guidelines for concrete mix design. *Indian Standard 10262-1982*.

Stone, W. C., Carino, N. J., & Reeve, C. P. (1986, September). Statistical methods for in-place strength predictions by the pullout test. In *Journal Proceedings* (Vol. 83, No. 5, pp. 745-756).

Table 1. Mix proportions considered in the present study

Mixture	Control	5% SF	10% SF	15%SF	20% SF	25% SF	30% SF
Cement (kg/m^3)	308	322	305	288	272	254	237
Silica fume (kg/m^3)	-	16.8	33.8	50.8	67.8	84.8	101.8
Natural sand (kg/m^3)	715	702	700	698	695	694	692
Coarse aggregate (kg/m^3)	1304	1281	1278	1274	1269	1266	1262
w/c	0.48	0.43	0.43	0.43	0.43	0.43	0.43
Water (kg/m^3)	148	148	148	148	148	148	148
Admixture (kg/m^3)	1.23	2.71	3.05	3.39	3.73	4.07	4.41

*Conversion factor kg/m^3= multiply by 0.062428 lb/ft^3

Table 2. Chemical and physical properties of Portland Slag Cement

Chemical Requirements	Test Results	Requirement as per IS:455-1989
Insoluble Residue (% by mass)	2.0	4.0 (Max)
MgO % by mass	6.7	10.0 (Max)
SO3 %by mass	1.8	3.0 (Max)
S % by mass	0.2	1.5 (Max)
Physical Requirements		
Specific Surface (blane) m^2/kg	343	225 (Min)
Specific Gravity	3.01	

Table 3. Chemical and physical properties of Silica Fume

Parameter	Specification	Analysis
Chemical Requirements		
SiO_2 %	85.0 (Min)	88.42
Moisture Content %	3.0 (Max)	0.15
Loss of Ignition %	6.0 (Max)	1.50
Physical Requirements		
>45 Micron %	10 (Max)	0.72
Pozzolanic Activity Index(7d) %	105 (Min)	137
Specific Surface (m^2/g)	15 (Min)	19.5
Bulk Density (kg/m^3)	500-700	615

Table 4. Compressive Strength, Flexural Strength and Tensile Splitting Strength of SF Concrete

Specimen	Compressive Strength (MPa)			Flexural Strength (MPa)			Tensile Splitting Strength (MPa)		
	Mean	SD	Range	Mean	SD	Range	Mean	SD	Range
Control	30.37	2.71	24.18-34.60	6.32	0.33	5.94-6.82	2.60	0.23	2.18-2.96
5% SF	30.73	4.17	18.73-38.01	6.39	0.74	4.10-7.44	3.02	0.31	2.51-3.60
10% SF	43.97	3.79	37.46-50.98	6.60	0.50	5.66-7.41	3.02	0.30	2.50-3.62
15% SF	47.42	6.29	37.75-60.82	6.62	0.29	6.05-7.02	3.59	0.46	2.85-4.33
20% SF	53.97	6.18	43.71-62.86	7.10	0.31	6.56-7.51	3.91	0.31	3.44 4.33
25% SF	49.06	5.96	41.26-62.52	8.35	0.48	7.36-9.10	3.78	0.38	3.14-4.32
30% SF	45.11	8.03	29.94-62.30	7.46	0.26	7.13-7.94	3.80	0.45	3.17-4.51

*Conversion factor MPa= multiply by 0.1450 ksi

Table 5. Estimated Parameters, KS Distances, LK, and CS for Different Distribution Functions describing Compressive Strength

Mix Name	Distribution	Shape	Scale	KS	CS	LK
Control	**Weibull**	13.49	31.57	0.077	0.648	-71.49
	Gamma	125.85	0.2414	0.073	0.88	-72.37
	Normal	30.376	2.717	0.062	0.713	-72.05
	Lognormal	0.091	30.23	0.072	0.76	-72.58
5% SF	**Weibull**	8.96	32.47	0.076	1.83	-84.04
	Gamma	51.31	0.59	0.077	1.70	-86.06
	Normal	30.738	4.179	0.067	1.77	-84.97
	Lognormal	0.146	30.416	0.082	1.36	-86.81
10% SF	Weibull	12.56	45.73	0.164	2.29	-83.58
	Gamma	140.35	0.313	0.147	0.90	-81.84
	Normal	43.97	3.797	0.151	0.97	-82.09
	Lognormal	0.085	43.816	0.141	0.70	-81.75
15% SF	Weibull	8.136	50.211	0.188	3.22	-98.61
	Gamma	59.706	0.794	0.167	0.99	-96.83
	Normal	47.425	6.298	0.175	1.49	-97.27
	Lognormal	0.131	46.993	0.157	0.79	-96.70
20% SF	**Weibull**	11.181	66.387	0.179	2.27	-95.01
	Gamma	77.657	0.692	0.204	4.06	-96.69
	Normal	53.773	6.091	0.183	3.07	-96.27
	Lognormal	0.116	53.410	0.192	3.75	-96.97
25% SF	Weibull	8.418	51.76	0.386	2.72	-97.92
	Gamma	72.55	0.676	0.412	0.41	-94.96
	Normal	49.067	5.963	0.406	0.79	-95.63
	Lognormal	0.118	48.715	0.409	0.33	-94.70
30% SF	**Weibull**	6.29	48.425	0.448	0.84	-104.99
	Gamma	31.425	1.435	0.446	1.88	-104.80
	Normal	45.114	8.039	0.444	1.44	-104.59
	Lognormal	0.1843	44.389	0.433	1.92	-105.13

Table 6. Estimated Parameters, KS Distances, LK, and CS for Different Distribution Functions describing Flexural Strength

Mix Name	Distribution	Shape	Scale	KS	CS	LK
Control	Weibull	22.707	6.477	0.142	-	-5.761
	Gamma	374.401	0.016	0.105	-	-6.001
	Normal	6.326	0.333	0.106	-	-5.919
	Lognormal	0.0532	6.296	0.097	-	-6.071
5% SF	**Weibull**	11.376	6.695	0.080	-	-20.344
	Gamma	67.395	0.094	0.121	-	-23.293
	Normal	6.398	0.074	0.086	-	-22.093
	Lognormal	0.129	6.347	0.114	-	-24.023
10% SF	Weibull	16.135	6.827	0.152	-	-13.641
	Gamma	178.158	0.037	0.117	-	-14.274
	Normal	6.606	0.502	0.118	-	-14.109
	Lognormal	0.077	6.586	0.106	-	-14.394
15% SF	**Weibull**	28.821	6.757	0.118	-	-2.436
	Gamma	529.181	0.012	0.137	-	-3.463
	Normal	6.621	0.293	0.155	-	-3.343
	Lognormal	0.044	6.612	0.159	-	-3.540
20% SF	**Weibull**	30.797	7.239	0.107	-	-2.949
	Gamma	520.572	0.013	0.526	-	-5.100
	Normal	7.107	0.315	0.155	-	-4.824
	Lognormal	0.045	7.113	0.163	-	-5.171
25% SF	**Weibull**	21.944	8.567	0.147	-	-12.472
	Gamma	300.758	0.027	0.529	-	-13.749
	Normal	8.353	0.488	0.143	-	-13.530
	Lognormal	0.059	8.39	0.143	-	-13.886
30% SF	Weibull	30.725	7.587	0.123	-	-2.405
	Gamma	829.575	0.009	0.135	-	-1.358
	Normal	7.46	0.266	0.123	-	-1.402
	Lognormal	0.0356	7.455	0.125	-	-1.351

Table 7. Estimated Parameters, KS Distances, LK, and CS for Different Distribution Functions describing Tensile Splitting Strength

Mix Name	Distribution	Shape	Scale	KS	CS	LK
Control	Weibull	13.597	2.707	0.107	-	-1.457
	Gamma	123.064	0.212	0.110	-	-0.653
	Normal	2.604	0.237	0.102	-	-0.873
	Lognormal	0.0933	2.585	0.102	-	-0.503
5% SF	Weibull	10.213	10.213	0.186	-	-5.969
	Gamma	99.679	0.03	0.106	-	-4.525
	Normal	3.302	0.313	0.159	-	-4.675
	Lognormal	0.1025	3.007	0.141	-	-4.336
10% SF	Weibull	10.467	3.161	0.14	-	-5.465
	Gamma	103.881	0.029	0.07	-	-4.006
	Normal	3.022	0.306	0.09	-	-4.217
	Lognormal	0.1005	3.007	0.08	-	-3.957
15% SF	Weibull	8.773	3.795	0.154	-	-13.118
	Gamma	61.461	0.058	0.122	-	-12.656
	Normal	3.591	0469	0.143	-	-49.661
	Lognormal	0.1312	3.560	0.131	-	-12.668
20% SF	**Weibull**	15.074	4.055	1.588	-	-4.683
	Gamma	158.572	0.0247	1.626	-	-4.968
	Normal	3.913	0.317	1.56	-	-4.929
	Lognormal	0.081	3.900	1.557	-	-5.020
25% SF	**Weibull**	12.305	3.949	0.12	-	-8.182
	Gamma	98.141	0.038	0.12	-	-9.053
	Normal	3.782	0.386	0.11	-	-8.842
	Log Normal	0.104	3.762	0.11	-	-9.206
30% SF	Weibull	9.739	4.005	0.159	-	-12.301
	Gamma	74.27	0.057	0.106	-	-11.951
	Normal	3.806	0.452	0.135	-	-12.023
	Lognormal	0.119	3.781	0.119	-	-11.971

Table 8. Most Appropriate Statistical Distribution Functions for Mechanical Properties of SF Concrete

Dosage of SF (%)	Compressive Strength	Flexural Strength	Tensile Splitting
0	Weibull (13.490, 31.570)	Lognormal (0.053, 6.296)	Lognormal (0.093, 2.585)
5	Weibull (8.960, 32.470)	Weibull (11.376, 6.695)	Gamma (99.679, 0.030)
10	Lognormal (0.085, 43.816)	Lognormal (0.077, 6.586)	Lognormal (0.101, 3.007)
15	Lognormal (0.131, 46.993)	Weibull (28.821, 6.757)	Gamma (61.461, 0.058)
20	Weibull (11.181, 66.387)	Weibull (30.797, 7.239)	Weibull (15.074, 4.055)
25	Lognormal (0.118, 48.715)	Weibull (21.944, 8.567)	Weibull (12.305, 3.949)
30	Weibull (6.290, 48.425)	Lognormal (0.036, 7.455)	Gamma (74.270, 0.057)

Note: The figures in the bracket denote the shape and scale parameters of each distribution respectively

Table 9. Design details of the selected building frame

Member	Floor no./ Storey no.	Width (mm)	Depth (mm)	Longitudinal Reinforcement detail	Transverse Reinforcement detail
Beam	1 to 3	300	450	[5-25 φ] (Top) + [4-20 φ] (Bottom)	10 φ@100 c/c
Beam	4	300	450	[5-25 φ] (Top) + [4-16 φ] (Bottom)	10 φ@100 c/c
Column	1-4	350	350	8-25 φ (Uniformly distributed)	10 φ@175 c/c

Table 10. Details of random variables used

Random variables	Mean	COV (%)	Probability Distribution	Source
Concrete compressive strength	33.66 MPa	21.0	Normal	Ranganathan (1999)
Steel yield strength	483.47 MPa	10.0	Normal	Ranganathan (1999)
Global damping ratio	5 %	76.0	Lognormal	Celik and Ellingwood (2009)

Table 11. Compressive strength of concrete of various buildings

Frame ID	Mean (MPa / %)	C.O.V (%)	Distribution	Source
C	30.28	8.94	Lognormal	Present study
SF5	30.73	13.56	Lognormal	Present study
SF10	43.97	8.61	Lognormal	Present study
SF15	47.42	13.26	Lognormal	Present study
SF20	53.97	11.45	Lognormal	Present study
SF25	49.06	12.14	Lognormal	Present study
SF30	45.11	17.80	Lognormal	Present study

Table 12. PSDM models for all the frames

Frame ID	$a(PGA)^b$	a	b
C	$2.58(PGA)^{0.62}$	2.58	0.62
SF5	$2.45(PGA)^{0.61}$	2.45	0.61
SF10	$2.92(PGA)^{0.79}$	2.92	0.79
SF15	$2.84(PGA)^{0.80}$	2.84	0.80
SF20	$3.26(PGA)^{0.86}$	3.26	0.86
SF25	$2.77(PGA)^{0.77}$	2.77	0.77
SF30	$3.06(PGA)^{0.81}$	3.06	0.81

Table 13. Reliability index (P_f) for SF building frames

Frame ID	PO-II, β_{Pf} (P_f)	PO-III, β_{Pf} (P_f)
C	1.07 (1.423E-01)	1.76 (3.920E-02)
SF5	1.14 (1.271E-01)	1.85 (3.216E-02)
SF10	1.39 (8.226E-02)	1.98 (2.385E-02)
SF15	1.42 (7.780E-02)	2.00 (2.275E-02)
SF20	1.41 (7.927E-02)	1.95 (2.559E-02)
SF25	1.42 (7.780E-02)	2.03 (2.118E-02)
SF30	1.14 (1.271E-01)	1.68 (4.648E-02)

APPENDIX

Table 1A. Compressive Strength of SF Concrete (in MPa)

Sl. No.	Control	5% SF	10% SF	15% SF	20% SF	25% SF	30% SF
1	24.18	18.73	37.46	37.75	43.71	41.26	29.94
2	26.23	25.42	39.56	38.77	43.74	41.41	30.54
3	26.66	25.78	39.68	39.39	44.37	41.52	34.07
4	26.76	26.29	39.98	39.48	44.78	42.34	34.15
5	27.26	26.55	40.21	41.08	45.23	42.57	34.22
6	27.41	26.57	40.43	41.29	46.81	43.18	37.84
7	27.81	26.68	40.50	42.70	46.84	44.21	39.38
8	28.54	27.34	40.51	43.44	48.23	44.26	40.50
9	28.64	29.11	40.72	43.52	48.28	44.47	40.71
10	28.84	29.18	41.29	43.89	48.83	46.01	41.19
11	29.21	29.23	41.71	44.24	51.78	46.03	41.19
12	29.72	29.55	41.74	44.32	52.51	46.13	44.27
13	29.83	29.64	41.86	44.38	54.47	46.18	44.50
14	30.22	30.02	42.15	44.49	55.88	46.24	44.61
15	30.51	30.46	42.81	44.56	56.77	46.77	45.81
16	30.98	31.59	43.65	45.27	57.51	48.16	46.65
17	31.17	32.14	43.88	45.82	57.59	49.68	46.71
18	31.34	32.53	44.55	47.30	58.17	50.12	47.05
19	31.52	32.91	45.16	50.15	58.25	50.34	48.10
20	31.56	33.15	45.40	50.35	58.28	50.66	48.11
21	31.82	33.30	46.80	51.76	58.34	51.59	48.26
22	32.57	33.44	47.17	52.64	58.38	53.12	49.18
23	32.81	33.45	47.36	53.61	58.41	53.16	49.78
24	32.81	33.64	47.53	53.64	58.69	53.28	50.74
25	32.85	34.55	47.93	54.40	58.86	54.35	50.75
26	33.28	34.63	48.98	54.83	58.97	56.06	52.33
27	33.57	35.25	49.17	55.27	59.89	56.13	53.65
28	34.11	35.46	49.72	56.29	60.54	58.96	57.86
29	34.29	37.43	50.14	57.18	62.12	61.17	58.92
30	34.60	38.01	50.98	60.82	62.86	62.52	62.30
Mean	30.37	30.73	43.97	47.42	53.97	49.06	45.11
SD	2.71	4.17	3.79	6.29	6.18	5.96	8.03

*Conversion factor MPa= multiply by 0.1450 ksi

Table 2A. Flexural Strength (MPa) of SF Concrete

Sl No.	Control	5% SF	10% SF	15% SF	20% SF	25% SF	30% SF
1	5.94	7.01	6.86	6.32	7.12	7.87	7.15
2	6.12	5.94	7.01	6.51	7.25	8.81	7.62
3	6.47	5.98	6.54	6.48	7.23	8.75	7.13
4	6.81	4.10	6.31	6.92	6.71	7.93	7.73
5	6.06	5.73	5.88	6.56	6.58	8.43	7.94
6	6.65	5.87	6.23	6.14	6.56	8.15	7.50
7	6.16	7.42	6.27	6.78	7.16	8.21	7.66
8	5.96	6.58	6.65	6.24	7.23	8.75	7.40
9	6.82	6.41	5.75	6.05	7.49	8.50	7.31
10	6.52	6.54	7.09	6.87	6.85	9.10	7.89
11	5.63	6.53	7.24	6.82	7.41	7.36	7.23
12	6.47	6.11	5.66	6.80	7.33	8.81	7.08
13	6.15	7.14	7.41	6.59	7.25	8.75	7.15
14	6.70	5.82	6.90	6.81	7.51	8.43	7.62
15	5.87	6.17	6.72	6.99	7.30	8.15	7.66
16	6.65	7.03	6.25	6.78	7.11	7.36	7.40
17	6.19	6.75	6.94	6.27	6.46	8.81	7.31
18	6.50	6.69	7.05	7.02	7.15	8.75	7.50
19	6.34	7.44	6.28	6.88	7.41	7.93	7.73
20	6.41	6.63	6.99	6.51	6.96	8.15	7.13
Mean	6.32	6.39	6.60	6.62	7.10	8.35	7.46
SD	0.33	0.74	0.50	0.29	0.31	0.48	0.26

*Conversion factor MPa= multiply by 0.1450 ksi

Table 3A. Tensile Splitting Strength (MPa) of SF Concrete

Sl. No.	Control	5% SF	10% SF	15% SF	20% SF	25% SF	30% SF
1	2.21	2.51	2.50	2.85	3.44	3.14	3.17
2	2.69	2.57	2.60	2.95	3.48	3.17	3.20
3	2.64	2.66	2.67	2.99	3.52	3.24	3.24
4	2.71	2.75	2.73	3.17	3.54	3.28	3.27
5	2.67	2.81	2.79	3.20	3.57	3.36	3.31
6	2.57	2.85	2.83	3.22	3.61	3.53	3.48
7	2.46	2.88	2.86	3.27	3.71	3.57	3.52
8	2.54	2.91	2.90	3.28	3.74	3.69	3.55
9	2.67	2.93	2.94	3.48	3.76	3.78	3.58
10	2.26	2.95	2.97	3.51	3.79	3.81	3.83
11	2.61	2.96	3.02	3.53	4.06	3.86	3.86
12	2.29	2.97	3.05	3.59	4.10	3.92	3.89
13	2.73	3.02	3.08	3.83	4.14	3.96	3.96
14	2.85	3.08	3.10	3.90	4.17	4.03	4.11
15	2.18	3.17	3.17	3.92	4.18	4.12	4.14
16	2.81	3.27	3.20	4.10	4.21	4.15	4.26
17	2.35	3.39	3.32	4.15	4.24	4.19	4.33
18	2.88	3.51	3.48	4.22	4.27	4.20	4.39
19	2.90	3.55	3.53	4.24	4.30	4.21	4.44
20	2.96	3.60	3.62	4.33	4.33	4.32	4.51
Mean	2.60	3.02	3.02	3.59	3.91	3.78	3.80
SD	0.23	0.31	0.30	0.46	0.31	0.38	0.45

*Conversion factor MPa= multiply by 0.1450 ksi

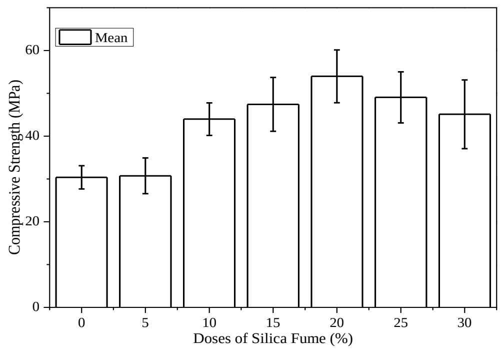

Fig. 1. Variation of Mean, SD of Compressive Strength (Conversion factor MPa= multiply by 0.1450 ksi)

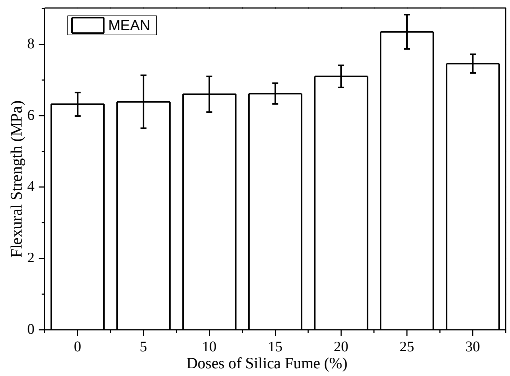

Fig. 2. Variation of Mean, SD of Flexural Strength (Conversion factor MPa= multiply by 0.1450 ksi)

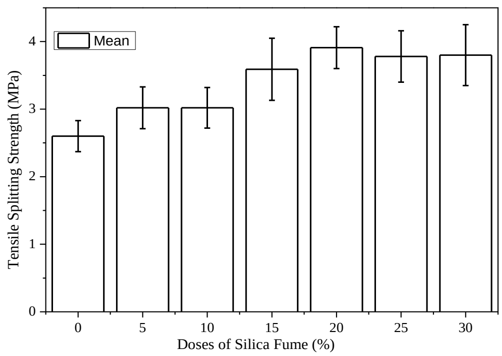

Fig.3. Variation of Mean, SD of Tensile Strength (Conversion factor MPa= multiply by 0.1450 ksi)

Fig. 4

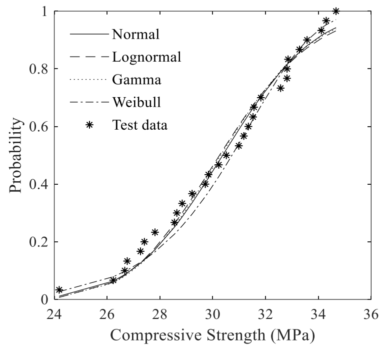

(a) Control

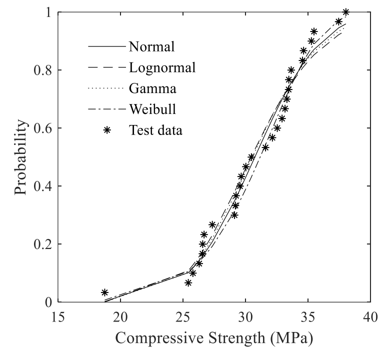

(b) 5% SF

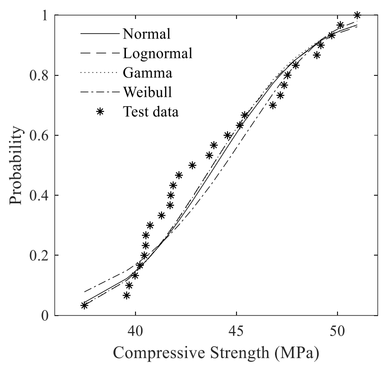

(c) 10% SF

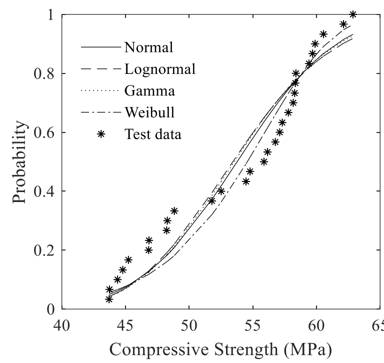

(d) 15% SF

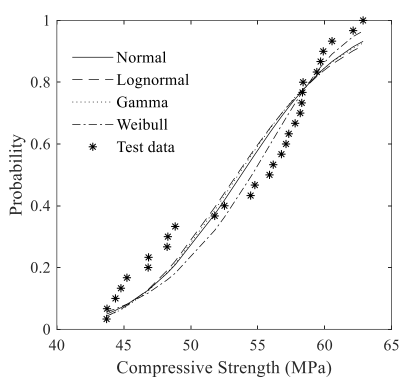

(e) 20% SF

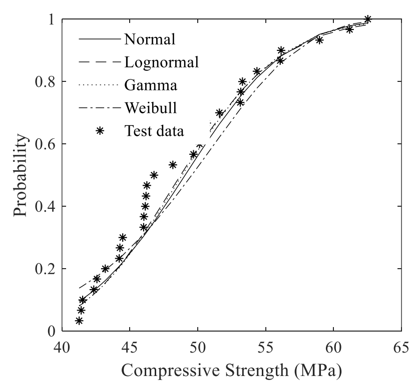

(f) 25% SF

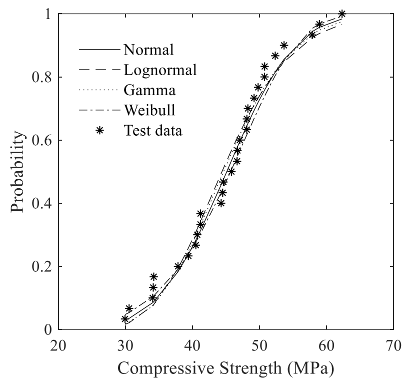

(g) 30% SF

Fig. 4. Experimental and Cumulative probability distributions for compressive strength (Conversion factor MPa= multiply by 0.1450 ksi)

Fig. 5

Click here to access/download;Figure;Figure 5.pdf

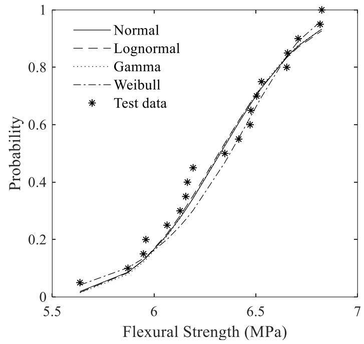

(a) Control

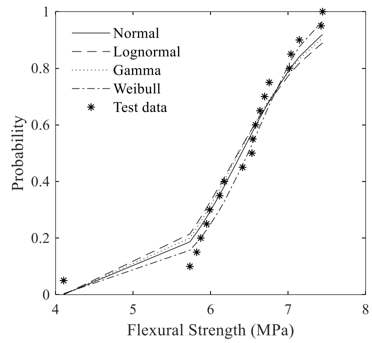

(b) 5% SF

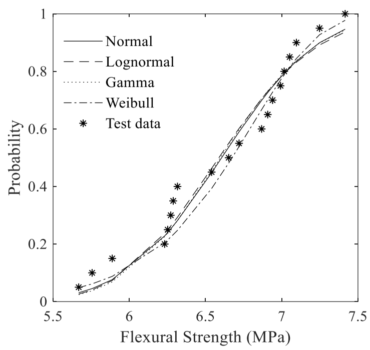

(c) 10% SF

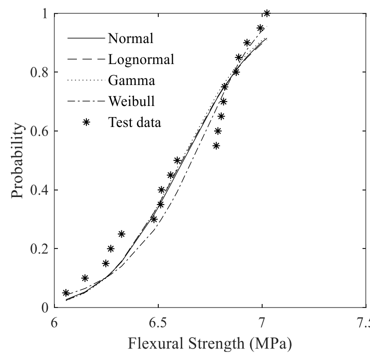

(d) 15% SF

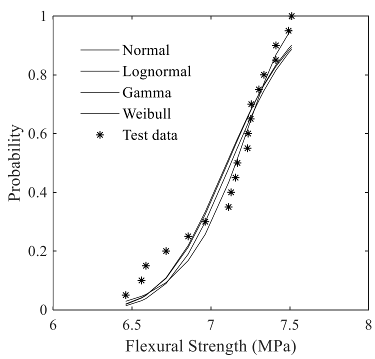

(e) 20% SF

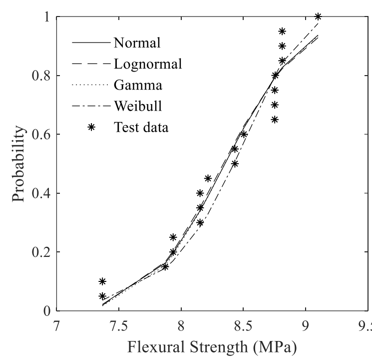

(f) 25% SF

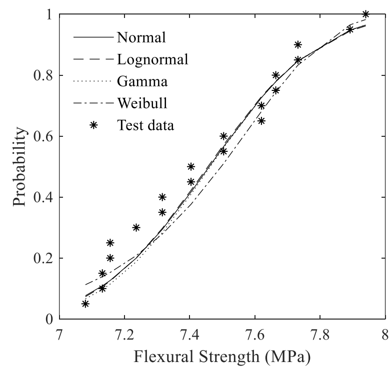

(g) 30% SF

Fig. 5. Experimental and Cumulative probability distributions for flexural strength (Conversion factor MPa= multiply by 0.1450 ksi)

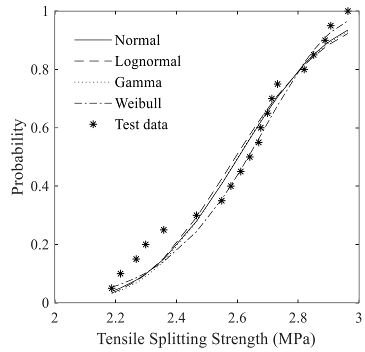

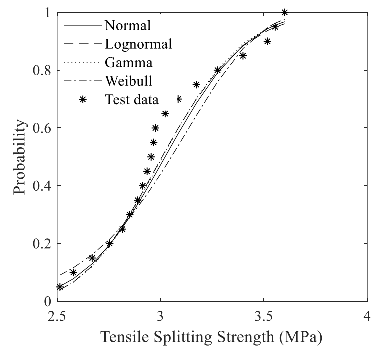

(a) Control (b) 5%

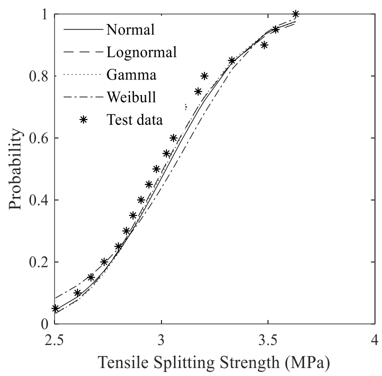

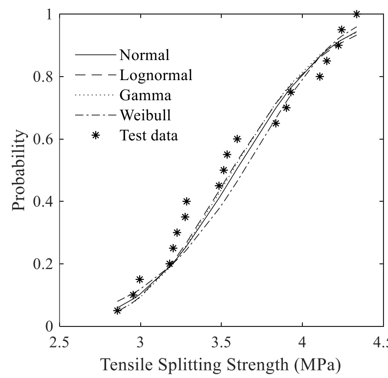

(c) 10% SF (d) 15% SF

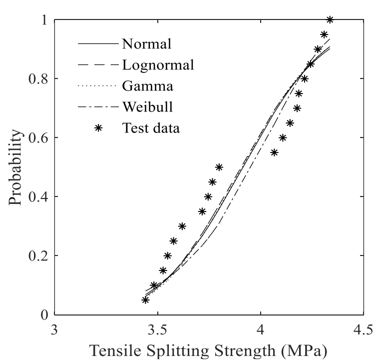

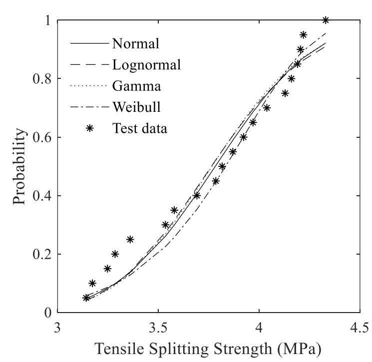

(c) 20% SF (d) 25% SF

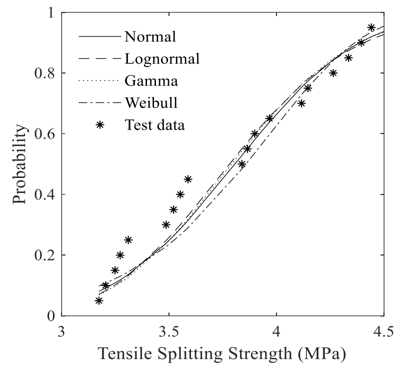

(d) 30% SF

Fig. 6. Experimental and Cumulative Probability Distributions for Tensile Splitting Strength (Conversion factor MPa= multiply by 0.1450 ksi)

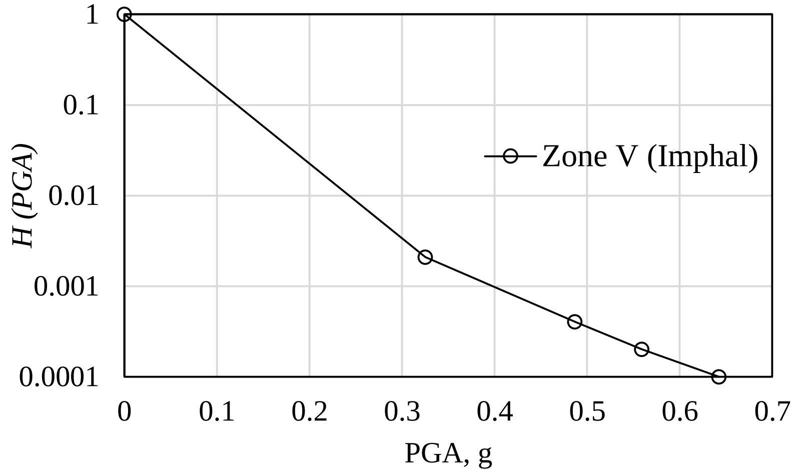

Fig. 7: Selected seismic hazard curves (data from Iyengar *et al*. 2010)

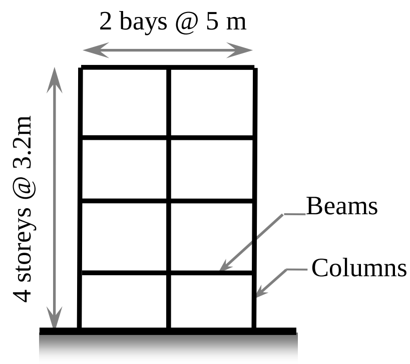

Fig. 8: Selected four storey RC frame

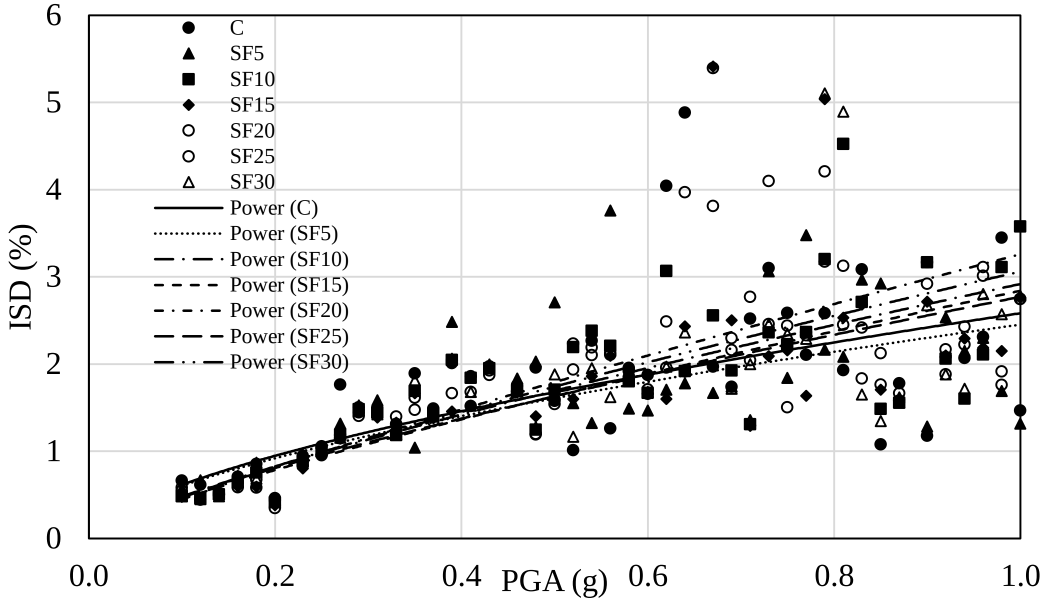

Fig. 9: PSDM models for building frames using SF concrete

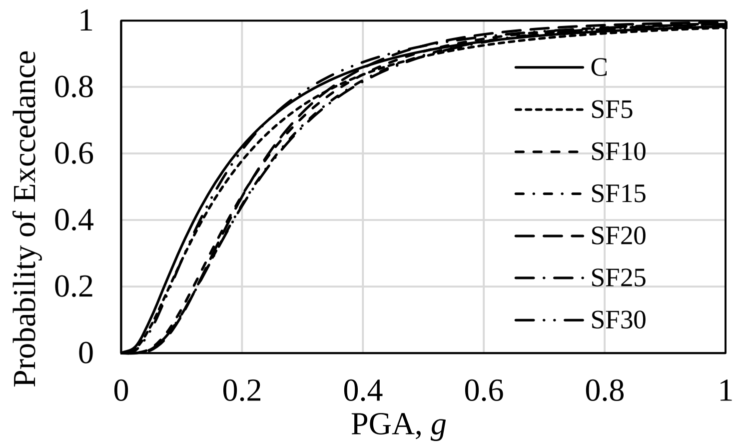

(a) At Significant Damage (SD)

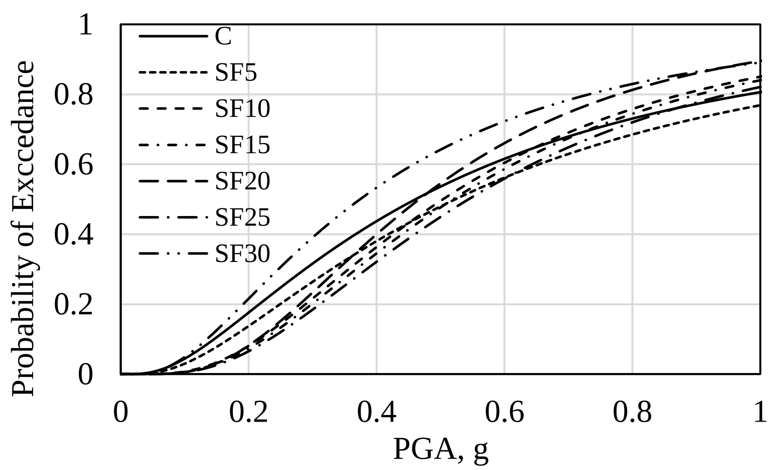

(b) At Collapse Prevention (CP)

Fig. 10: Fragility curves for SF building frames

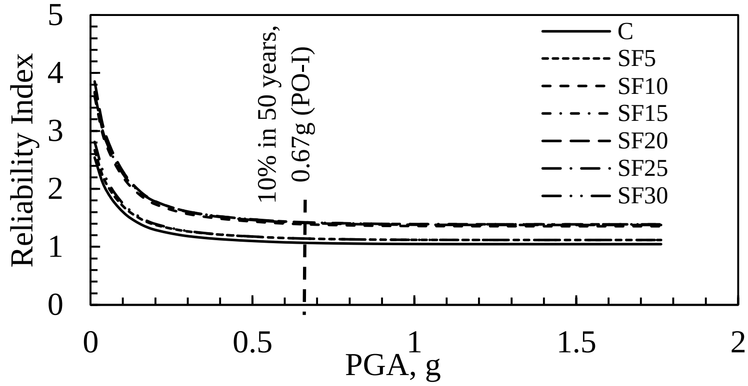

(a) At SD for SF building frames

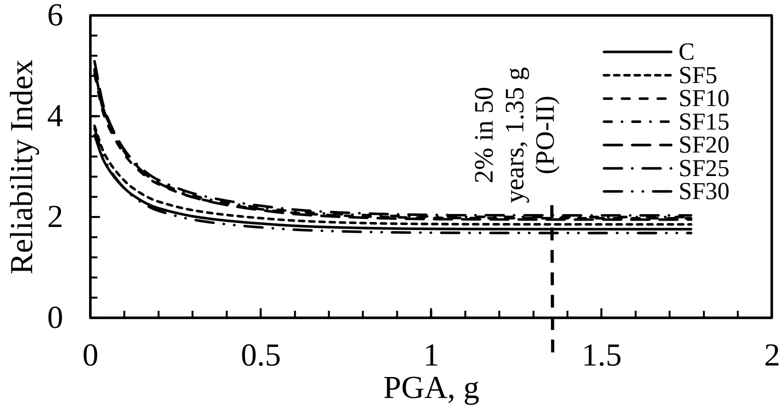

(b) At CP for SF building frames

Fig. 11: Reliability curves for SF building frames

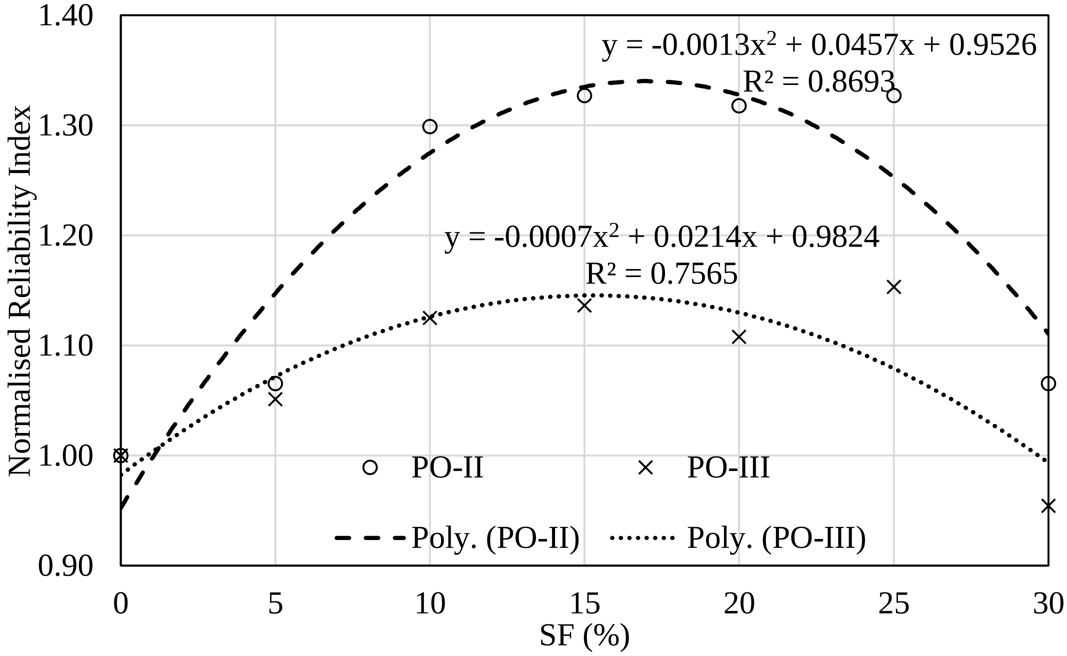

Fig. 12: Percentage of SF versus normalized reliability index

Fig. 1. Variation of Mean, SD of Compressive Strength (Conversion factor MPa= multiply by 0.1450 ksi)

Fig. 2. Variation of Mean, SD of Flexural Strength (Conversion factor MPa= multiply by 0.1450 ksi)

Fig.3. Variation of Mean, SD of Tensile Strength (Conversion factor MPa= multiply by 0.1450 ksi)

Fig. 4. Experimental and Cumulative probability distributions for compressive strength (Conversion factor MPa= multiply by 0.1450 ksi)

Fig 4 (a) Control

Fig 4 (b) 5% SF

Fig 4 (c) 10% SF

Fig 4 (d) 15% SF

Fig 4 (e) 20% SF

Fig 4 (f) 25% SF

Fig 4 (g) 30% SF

Fig. 5. Experimental and Cumulative probability distributions for flexural strength (Conversion factor MPa= multiply by 0.1450 ksi)

Fig 5 (a) Control

Fig 5 (b) 5% SF

Fig 5 (c) 10% SF

Fig 5 (d) 15% SF

Fig 5 (e) 20% SF

Fig 5 (f) 25% SF

Fig 5 (g) 30% SF

Fig. 6. Experimental and Cumulative Probability Distributions for Tensile Splitting Strength (Conversion factor MPa= multiply by 0.1450 ksi)

Fig 6 (a) Control

Fig 6 (b) 5% SF

Fig 6 (c) 10% SF

Fig 6 (d) 15% SF

Fig 6 (e) 20% SF

Fig 6 (f) 25% SF

Fig 6 (g) 30% SF

Fig. 7: Selected seismic hazard curves (data from Iyengar *et al*. 2010)

Fig. 8: Selected four storey RC frame

Fig. 9: PSDM models for building frames using SF concrete

Fig. 10: Fragility curves for SF building frames

Fig 10 (a) At Significant Damage (SD)

Fig 10 (b) At Collapse Prevention (CP)

Fig. 11: Reliability curves for SF building frames

Fig 11(a) At SD for SF building frames

Fig 11(b) At CP for SF building frames

Fig. 12: Percentage of SF versus normalized reliability index